

Published in final edited form as:

Nat Neurosci. 2013 December ; 16(12): 1731–1733. doi:10.1038/nn.3573.

Independent hypothalamic circuits for social and predator fear

Bianca A. Silva¹, Camilla Mattucci¹, Piotr Krzywkowski¹, Emanuele Murana², Anna Illarionova³, Valery Grinevich³, Newton S. Canteras⁴, Davide Ragozzino², and Cornelius T. Gross^{1,*}

¹Mouse Biology Unit, European Molecular Biology Laboratory (EMBL), via Ramarini 32, 00015 Monterotondo, Italy

²Pasteur Institute – Foundation Cenci Bolognetti and Department of Human Physiology and Pharmacology, Center of Excellence BEMM, University of Rome – La Sapienza, Piazzale Aldo Moro 5, 00185 Rome, Italy

³Schaller Research Group on Neuropeptides, German Cancer Research Center DKFZ, CellNetwork Cluster of Excellence, University of Heidelberg, Im Neuenheimer Feld 581, 69120 Heidelberg, Germany

⁴Department of Anatomy, Institute of Biomedical Sciences, University of São Paulo, Av. Professor Lineu Prestes 2465, 05508 São Paulo, Brazil

Abstract

The neural circuits mediating fear to naturalistic threats are poorly understood. Here we demonstrate that functionally independent populations of neurons in the ventromedial hypothalamus (VMH), a region implicated in feeding, sex, and aggression, are essential for predator and social fear in mice. Our study establishes a critical role for VMH in fear and carries implications for the selective intervention in pathological fear in humans.

Studies in laboratory animals have routinely used freezing behavior elicited by exposure to cues associated with electric foot shock to study the neural circuits underlying fear. However, evidence suggests that fear behaviors elicited by other types of threat may not depend on these circuits ¹. In particular, c-Fos mapping studies have shown that exposure to a predator or an aggressive conspecific recruit the medial hypothalamus, a region implicated in motivated behaviors such as feeding, sex, and aggression ². Intriguingly, exposure to predator and aggressive conspecific activate non-overlapping nuclei in the medial hypothalamus suggesting that predator and social fear may depend on separate circuits ³. However, it remains unclear whether the different brain regions recruited by foot shock,

*to whom correspondence should be addressed: gross@embl.it.

Author Contributions

B.A.S. designed, carried out, and analyzed all experiments, except for some behavioral experiments that were carried out and analyzed by C.M. and P.K. and the electrophysiology experiments that were designed, carried out, and analyzed by E.M. and D.R. Viruses were produced and tested by A.I. and V.G. The project was conceived by B.A.S. and C.T.G. with critical input from N.S.C. The manuscript was written by B.A.S. and C.T.G. with input from D.R. and N.S.C.

Competing financial interests

The authors declare no competing financial interests.

predator, and aggressive conspecific reflect truly independent fear circuits or arise as a result of differences in the behaviors elicited, differences between innate and learned fear, or differences in testing methodology.

We developed a behavioral test in which similar patterns of fear behavior are elicited in mice by exposure to either a predatory rat, an aggressive mouse, or an electric foot shock (Fig. 1a). The apparatus consisted of two chambers separated by a narrow corridor. Mice were housed in one chamber and each day a door was opened to allow brief access to the corridor and second chamber. On the fourth day the mouse was confined to the second chamber and briefly exposed to a predatory rat, an aggressive conspecific, a foot shock, or a fake toy rat. The door was reopened and defensive behaviors (immobility, flight, stretch postures, locomotion) were recorded. On the following day mice were again allowed free access to the corridor and second chamber in the absence of threat and defensive behaviors were scored as a measure of contextual fear. Mice showed a significant increase in stretch postures, immobility, and flight and decrease in locomotion following exposure to all threats when compared to their behavior during habituation (Fig. 1b–d and S1). Exposure to the conditioned context also elicited a significant increase in stretch postures, immobility, and flight and decrease in locomotion (Figure 1b–d and S1), while exposure to a toy rat did not elicit significant increases in stretch postures, immobility, or flight, but did result in a significant decrease in locomotion following acute exposure suggesting that some of the decreased locomotion to threat is due to the novelty of the stimulus. These data validate our test as a robust method to examine similar acute and learned fear responses to foot shock, predator, and social threat.

To investigate whether distinct neural activation patterns are induced by foot shock, predator, and aggressive conspecific under conditions of similar testing methodology and behavior we performed c-Fos mapping in our test. C-Fos was induced in different brain regions in accordance with previous reports [2, 3]. In particular, predator exposure significantly activated the dorsomedial division of the VMH (VMHdm), while exposure to an aggressive conspecific significantly activated the ventrolateral VMH (VMHvl, Fig. 1e–g). Neither control mice nor mice exposed to foot shock showed activation in VMH, demonstrating that the medial hypothalamus is selectively recruited during predator and social fear, and that similar fear behaviors recruit different brain circuits. Notably, these data suggest that VMHdm, a region extensively implicated in the control of energy homeostasis and metabolism⁴, has a role in predator fear, while VMHvl, a region previously implicated in sexual and aggressive behavior^{4–7}, has a role in social fear.

To test whether VMH harbors functionally independent circuits for predator and social fear we used the hM4D/CNO pharmacogenetic neural inhibition tool⁸ to rapidly and selectively inhibit neurons in VMHdm and VMHvl in behaving mice. Stable expression of hM4D in VMHdm neurons was achieved by constructing transgenic mice in which hM4D was driven by the *Nr5a1* gene promoter⁹ (*Nr5a1::hM4D-2A-TomatoF*, Fig. 2a). Reporter gene expression in the transgenic mice was found in the dorsomedial and central divisions of VMH, in VMH efferents of the supraoptic commissure, and in all known VMH target areas, including dorsal PAG¹⁰ (Fig. 2b–d and S2). Expression of hM4D was found selectively in *Nr5a1*-expressing neurons in the transgenic animals (Fig. 2e–g and S3). *In vitro* patch clamp

electrophysiology confirmed a significant reduction in spontaneous firing and membrane potential in VMHdm neurons in brain slices from transgenic (firing rate = $-32\% \pm 6$, $P < 0.01$, $N = 8$; membrane potential = $-3.35 \text{ mV} \pm 1.07$, $P < 0.01$, $N = 15$), but not non-transgenic littermates (firing rate = $7.6\% \pm 25.2$, $P > 0.05$, $N = 8$; membrane potential = $0.71 \text{ mV} \pm 0.94$, $P > 0.05$, $N = 10$) treated with clozapine-N-oxide (CNO), a selective agonist of hM4D that is otherwise biologically inert¹¹ (Fig. 2h). Systemic treatment of *Nr5a1::hM4D-2A-TomatoF* transgenic, but not non-transgenic littermate control mice with CNO prior to threat exposure caused a significant decrease in defensive behaviors and increase in locomotion to predator. Similar treatment had no effect on fear behaviors elicited by exposure to aggressive conspecific or foot shock (Fig. 3a, b). These data demonstrate that VMHdm has an essential and selective role in the expression of predator fear behavior.

Expression of hM4D in VMHvl neurons was achieved by local infection with adeno-associated virus (AAV) expressing hM4D (AAV-Syn::*Venus-2A-hM4D*, Fig. 3c, d S4a–f, S5a–f). CNO treatment of AAV-Syn::*Venus-2A-hM4D* infected mice prior to threat exposure caused a significant decrease in defensive behaviors and increase in locomotion to an aggressive conspecific when compared to vehicle treated controls, but no change in fear behavior elicited by predator (Fig. 3e, f). In some cases expression of hM4D in virally infected animals extended to the VMHdm (Fig. S5b) and tuberal nucleus (Fig. S5d) and we cannot completely rule out that inhibition of cells in these nuclei contributed to the behavioral effects seen. The observation that expression in these structures was significantly lower than in VMHvl (Fig. S5e) and that this infection was not associated with a reduction in predator fear, suggests that this ectopic expression was not sufficient to modulate fear behavior. Expression outside the VMH was sparse (Fig. S5c). Importantly, CNO treatment did not affect the number of attacks received nor the submissive behavior during the direct encounter with the aggressor (Fig. S6a, b). These data demonstrate a double dissociation of VMH circuits supporting fear behavior to predator and social threats.

Finally, we examined whether fear of predator, aggressive conspecific, and foot shock were also functionally dissociable at the level of the periaqueductal gray (PAG), a downstream structure involved in motor pattern initiation and shown to be critical for the expression of fear responses¹². Both VMHdm and VMHvl project prominently to the dorsal PAG (dPAG)¹⁰, and CNO-treated mice with local infection of AAV-Syn::*Venus-2A-hM4D* (Fig. 3g) in dPAG showed significantly reduced predator and social, but not foot shock fear when compared to vehicle-treated, similarly infected controls (Fig. 3h). Although CNO treatment did not affect the number of attacks received, a decrease in submissive behavior was observed during the direct encounter with the aggressor (Fig. S9a, b) suggesting that dPAG plays a role in supporting passive defensive behaviors during conspecific encounters. Although infection often included the overlying superior colliculus (SC, Fig. S7), treatment of mice explicitly infected in SC with CNO did not result in a change in fear behavior (Fig. S8). These data demonstrate that the neural circuits supporting defensive behaviors to distinct threats are also dissociable at the level of downstream motor initiation centers.

Our findings demonstrate that VMH is a multi-modal hub for the control of motivated behaviors and physiological homeostasis. *Nr5a1*-expressing cells in VMHdm are leptin responsive and essential for supporting metabolic responses to dietary challenge⁴ and our

data suggest that a link between metabolic regulation and predator fear may occur at the level of the VMHdm. Consistent with an evolutionarily conserved role for VMHdm in fear, electrical stimulation of VMHdm in humans elicits panic attacks¹³. On the other hand, the dual role of VMHvl in aggression^{5, 6} and social fear suggests that it functions as a key threat processing circuit during social encounters. Our observation that dPAG is critical for predator and social, but not foot shock fear further supports the existence of independent fear circuits at both the level of fear processing and expression. These data demonstrate that fear to different classes of threat are processed in distinct circuits and open the possibility for the selective pharmacological blockade of fear. Finally, our data provide the first functional dissection of the neural circuits supporting social fear, an important risk factor for mental illness.

Materials & Methods

Animals

All mice were derived from local EMBL breeding colonies. Non-transgenic experimental subjects were adult C57BL/6N mice. Predators were adult male SHR/NHsd rats (Harlan, Correzzana, Italy). Aggressive conspecifics were adult male CD1 mice selected for elevated aggression as previously described¹⁴. All animals were housed at 22–25 C on a 12 hour light-dark cycle with water and food *ad libitum*. Males were used for all experiments except for data in Fig. 3a, b where both males and females were tested. No sex difference in behavioral responses was observed. All animals were handled according to protocols approved by the Italian Ministry of Health (#231/2011-B, #121/2011-A).

Behavioral testing

The experimental apparatus (adapted from¹⁵) was made of clear Plexiglas and composed of similar detachable home and stimulus chambers (25 × 25 × 25 cm) that were connected by an opening (2.0 cm wide, 2.0 cm high) to a narrow corridor (12.5 cm wide, 60 cm long, 30 cm high). Both openings could be closed by a manual sliding door. The experimental subject was continuously housed in the home chamber with access to food and water for the entire test. Each day the home cage was carried from the housing room to the testing room and attached to the apparatus and the sliding door opened to give the mouse access to the entire apparatus for 20 minutes (habituation period). In case of foot shock, a metal grid connected to a scrambled electric shock generator (Med Associates, Berlin, VT) was placed into the stimulus compartment. On day 4, following 10 minutes of exploration, the experimental mouse was confined to the stimulus compartment by closing the door and either a rat or an aggressive mouse was placed into the stimulus compartment and allowed to interact (rat: <5 s, mouse: 10 min) before the door was re-opened to allow the experimental mouse to escape. The door was immediately re-closed in the case of the stimulus mouse to prevent escape. In case of foot shock, a scrambled electric current was delivered to the grid over a period of one minute (0.5 mA every 15 s) before the door was re-opened. To prevent injury to the experimental mouse the experimenter held the rat during the direct encounter. Defensive behaviors were scored during the first 3 minutes of free exploration each day and during the first 3 minutes of the post-stimulus period. Clozapine-N-oxide (3mg/kg i.p. in 0.9% saline; Enzo Life Sciences, Farmingdale, NY) or vehicle was injected 30 minutes before the

beginning of the test. On day 5 the experimental mouse was given access to the entire apparatus as on the habituation days. Between each subject the apparatus was cleaned first with 50% ethanol and then detergent and the bedding was changed. The apparatus was washed in an automatic cage washer between testing days to eliminate odors. All the testing was performed during the dark phase under red light illumination (40 W).

Animals were naïve to the testing apparatus except in the case of data included in Fig. 3e, f, h where predator and foot shock exposed mice had been previously tested. In these cases, pseudo-randomization of drug treatment groups was performed and no influence of multiple drug treatment was observed. Behavior was scored from videotape using Observer software (Noldus, Wageningen, Netherlands) by an experimenter blind to genotype and treatment. Behaviors were scored as follows – immobility: subject motionless, stretch postures: body stretched forward without movement or animal moving slowly towards stimulus compartment in an elongated posture, flight: subject quickly running toward home cage, locomotion: ambulatory movement not characterized by stretch posture. Defensive behavior was the sum of stretch postures and immobility. In the case of animals tested for social fear the number of biting attacks received and the time spent in an upright/submissive posture during the direct encounter was also scored. In two cases the experimental animal performed a significant number of attacks toward the intruder (>70% of all attacks) and was excluded from the analysis.

Statistical analysis

Data analysis was performed with PRISM software (GraphPad, San Diego, CA). All data are reported as mean \pm standard error measurement. Statistical significance was determined by repeated measures ANOVA with behavior during habituation, stimulus, and context considered as repeated measures coupled to Bonferroni *post hoc* analysis in case of significance (Fig. 1, S1), by t-test (Fig. 2–3, S5e, S6, S8, S9), or MANCOVA¹⁶ followed by pairwise correlation analysis (Fig. S5). In the *in vitro* electrophysiology experiments the changes from baseline in firing rate and membrane potential were calculated by t test. No statistical methods were used to predetermine group sizes. The sample sizes we chose are similar to those used in previous publications

Histology

C-Fos immunohistochemistry—Ninety minutes after exposure to the stimulus (predator, conspecific, or foot shock) the experimental mouse was deeply anesthetized with Avertin (Sigma-Aldrich, St. Louis, MO), perfused trans-cardially (4.0% paraformaldehyde, 0.1 M phosphate buffer, pH 7.4), and the brain removed, postfixed (4% PFA overnight), and cryoprotected (20% sucrose, PBS, 4 C, overnight). The brains were frozen and 40 μ m coronal sections were cut with a sliding cryostat (Leica Microsystems, Wetzlar, Germany) and processed for immunohistochemistry with rabbit anti-Fos antiserum (1:20,000, Ab-5, Calbiochem, San Diego, CA). The primary antiserum was localized using a variation of the avidin-biotin complex system (Vector Laboratories, Burlingame, CA;¹⁷). In brief, sections were incubated for 90 min at room temperature in a solution of biotinylated goat anti-rabbit IgG (Vector Laboratories) and then placed in the mixed avidin-biotin horseradish peroxidase complex solution (ABC Elite Kit, Vector Laboratories) for the same period of time. The

peroxidase complex was visualized by a 5 min exposure to chromogen solution (0.05 % 3,30-diaminobenzidine tetrahydrochloride [Sigma-Aldrich], 0.4 mg/ml nickel ammonium sulfate, 6 µg/ml glucose oxidase [Sigma-Aldrich], 0.4 mg/ml ammonium chloride in PBS) followed by incubation in the same solution with 2 mg/ml glucose to produce a blue-black product. The reaction was stopped by extensive washing in PBS. Sections were dehydrated and cover-slipped with quick mounting medium (Eukitt, Fluka Analytical, St. Louis, MO)

Fluorescent protein detection—Animals were trans-cardially perfused (4.0% paraformaldehyde, 0.1 M phosphate buffer, pH 7.4) and brains removed and left overnight in fixative. Coronal sections (70 µm) were cut on a vibratome (Leica Microsystems). All sections were imaged for Venus, TomatoF and DAPI fluorescence with a motorized wide-field microscope (Leica Microsystems).

Double immunostaining—Animals were perfused trans-cardially (4.0% paraformaldehyde, 0.1 M phosphate buffer, pH 7.4) and the brain removed, postfixed (4% PFA overnight), and cryoprotected (20% sucrose, PBS, 4 C, overnight). The brains were frozen and 40 µm coronal sections were cut with a sliding cryostat (Leica Microsystems) and processed for immunohistochemistry with anti-HA antibody raised in rat (1:200, 11867423001, Roche, Basel, Switzerland) and anti-Nr5a1 antibody raised in rabbit (1:200, K0611, Trans Genic Inc., Kumamoto, Japan). Before incubation with primary antibodies the sections were boiled for ten minutes in citrate buffer (10 mM) and incubated with blocking solution (1% BSA, 5% NGS in PBS and 0.4 % Triton-X) for one hour. Primary antibodies were detected with fluorescent-labeled secondary antibodies (1:800, Alexa Fluor 488 Goat Anti-Rabbit, A-11034; 1:800, Alexa Fluor 647 Goat Anti-Rat, A-21248, Invitrogen, Carlsbad, CA).

Generation of transgenic mice

Recombineering was used to insert a HA-hM4D-2A-TomF-FRT-kan/neo-FRT cassette replacing the translational start of the *Nr5a1* gene in a bacterial artificial chromosome (BAC) clone (RP23-225F7, CHORI-BACPAC, Oakland, CA). The hemagglutinin-tagged hM4D sequence (HA-hM4D) was excised from pcDNA-5FRT-HA-hM4D (gift of B. Roth, University of North Carolina, Chapel Hill, NC). A farnesylation domain (KLNPPDESGPGCMSCKCVLS¹⁸) was added to the C-terminus of the Tomato open reading frame and the viral P2A¹⁹ sequence was inserted between hM4D and TomatoF to produce separate peptides from a single open-reading frame. Modified BAC DNA was prepared (Large-construct kit, Qiagen, Valencia, CA), diluted in injection buffer (30 mM Tris-HCl pH 7.5, 0.1 mM EDTA, 100 mM NaCl), and microinjected into the pronucleus of fertilized one-cell stage B6x(B6xD2) embryos. One of two founders showed stronger reporter gene expression was used in all studies and backcrossed to C57BL/6N. Transgenic mice were genotyped by PCR (Forward: 5'-CAATCCAGCTGTGTGCCCTACTTCGCC-3', Reverse: 5'-GGCCATAGCGTAATCTGGAACATCGTATGGGTA-3')

In vitro Electrophysiology

Coronal slices (250 µm) containing the VMH were cut at 4 C using a vibratome (DSK, Dosaka EM, Kyoto, Japan) from brains incubated for 5–10 minutes in ice-cold oxygenated

modified artificial cerebrospinal fluid (mACSF: 3 mM KCl, 2 mM MgCl₂, 1.6 mM CaCl₂, 1.25 mM NaH₂PO₄, 2 mM MgSO₄, 26 mM NaHCO₃, 10 mM glucose, 200 mM sucrose) extracted from transgenic and control littermates anaesthetized with halothane and decapitated. Slices were maintained for at least 1 h at room temperature (22–25 C) in oxygenated (95% - 5% CO₂) ACSF (125 mM NaCl, 2.5 mM KCl, 2 mM CaCl₂, 1 mM MgCl₂, 1.25 mM NaH₂PO₄, 26 mM NaHCO₃, 10 mM glucose, pH 7.35). Recordings were performed at room temperature in ACSF perfused at a rate of ~ 1.5 ml/min. Clozapine-N-oxide (CNO, 10 μM) was applied to the slice by bath perfusion for 3 minutes. Whole-cell patch clamp recording in current clamp configuration were performed using borosilicate glass pipettes (3–5 MΩ) filled with 140 mM K-Gluconate, 2 mM MgCl₂, 5 mM BAPTA, 10 mM HEPES, 2 mM MgATP, 0.4 mM NaGTP, and pH corrected with KOH to pH 7.32. Recordings were performed using an Axopatch 200A amplifier (Molecular Devices, Foster City, CA); signal was low-pass filtered at 2 kHz, collected at 10 kHz using Clampex10 (Molecular Devices), and analyzed off-line with Clampfit10, software (Molecular Devices). In some experiments 10–50 pA of current were injected to induce firing. Recordings were discarded if membrane potential and/or firing rate were unstable. To determine changes in membrane potential, signals were digitized at 1 Hz, firing frequency was monitored using 30 s duration bins. In both cases, CNO response was assessed 4 minutes following the start of drug application.

Viral production

The Venus-P2A-HA-hM4D cassette was cloned so as to replace the open reading frame of pAAV-Syn-NpHR3.0-EYFP-WPRE (gift of K. Deisseroth, Stanford University, Palo Alto, CA). Production and purification of recombinant AAV (chimeric capsid serotype 1/2) were as described²⁰. Viral titers (>10¹⁰ genomic copies per μl) were determined with QuickTiter AAV Quantitation Kit (Cell Biolabs, San Diego, CA) and RT-PCR as previously described²¹.

Stereotaxic viral injections

Bilateral injection of AAV aimed at the VMHvl (posterior: –0.95 mm, depth: –5.75 mm, lateral: ±0.65 mm to bregma, coordinates empirically adapted from²²) or dorsal PAG (posterior: –3.8 mm, depth: –2.3 mm lateral ±1.0, angle: 26 degrees), were performed using a glass pipette (intraMARK, 10–20 μm tip diameter, Blaubrand, Wertheim, Germany) connected to a syringe and a stereotaxic micromanipulator (Kopf Instruments, Tujunga, CA) in deeply anaesthetized animals (Ketavet, Ketamine 100 mg/kg, Xylazine 10 mg/kg, Intervet, Segrate, Italy). We injected 0.3 μl of AAV-containing solution per side in VMHvl and 0.1 μl per side in dPAG. Behavioral experiments were performed 3–4 weeks after surgery.

Quantification of viral infection

The location of viral infection was determined in all animals injected with AAV. The animals were trans-cardially perfused with 4% paraformaldehyde within three days of behavioral testing. The exact position of the brain nucleus of interest was determined by overlaying a reference atlas grid²² using white matter landmarks onto the bright field fluorescent image. Venus signal was thresholded and quantified (ImageJ Software) and

infection efficiency (either % area or total area) was calculated over the total area of the nucleus as determined from the atlas overlay. Fifteen dPAG-infected animals that showed less than 10 % infection of the target area were excluded from the behavior analysis. No VMHvl-infected animals were excluded from the behavior analysis.

Supplementary Material

Refer to Web version on PubMed Central for supplementary material.

Acknowledgments

We would like to thank Francesca Zonfrillo and Raffaele Migliozi for expert mouse husbandry, Enrica Audero, Philip Hüblitz and the EMBL Transgenic Facility for help in producing the transgenic mouse line, the EMBL Mechanical Workshop for construction of the behavioral apparatus, Laura Carbonari for help with behavioral testing and histology, Mu Yang for advice on behavioral test design, Simone Motta for advice on c-Fos immunohistochemistry, Elena Amendola for the farnesylated tomato construct, Rocio Sotillo and Martin Jechlinger for the anti-HA and fluorescent secondary antibodies and Bernd Klaus for help in the statistical analysis. This work was supported by funds from NIH (MH093887-01) to C.T.G., from EMBL to C.T.G, B.A.S., P.K., and C.M., and from the German Research Foundation (DFG, GR 3619/2-1, 3619/3-1, GR 3619/4-1) and Chica and Heinz Schaller Research Foundation to V.G.

References

1. Gross CT, Canteras NS. *Nat Rev Neurosci.* 2012; 13:651–658. [PubMed: 22850830]
2. Canteras NS. *Pharmacol Biochem Behav.* 2002; 71:481–491. [PubMed: 11830182]
3. Motta SC, Goto M, Gouveia FV, Baldo MV, Canteras NS, Swanson LW. *Proceedings of the National Academy of Sciences of the United States of America.* 2009; 106:4870–4875. [PubMed: 19273843]
4. Dhillon H, Zigman JM, Ye C, Lee CE, McGovern RA, Tang V, Kenny CD, Christiansen LM, White RD, Edelstein EA, Coppari R, Balthasar N, Cowley MA, Chua S Jr, Elmquist JK, Lowell BB. *Neuron.* 2006; 49:191–203. [PubMed: 16423694]
5. Lin D, Boyle MP, Dollar P, Lee H, Lein ES, Perona P, Anderson DJ. *Nature.* 2011; 470:221–226. [PubMed: 21307935]
6. Kruk MR, Van der Poel AM, Meelis W, Hermans J, Mostert PG, Mos J, Lohman AH. *Brain Res.* 1983; 260:61–79. [PubMed: 6681724]
7. Simerly RB. *Annu Rev Neurosci.* 2002; 25:507–536. [PubMed: 12052919]
8. Armbruster BN, Li X, Pausch MH, Herlitze S, Roth BL. *Proceedings of the National Academy of Sciences of the United States of America.* 2007; 104:5163–5168. [PubMed: 17360345]
9. Kurrasch DM, Cheung CC, Lee FY, Tran PV, Hata K, Ingraham HA. *The Journal of neuroscience: the official journal of the Society for Neuroscience.* 2007; 27:13624–13634. [PubMed: 18077674]
10. Canteras NS, Simerly RB, Swanson LW. *The Journal of comparative neurology.* 1994; 348:41–79. [PubMed: 7814684]
11. Alexander GM, Rogan SC, Abbas AI, Armbruster BN, Pei Y, Allen JA, Nonneman RJ, Hartmann J, Moy SS, Nicolelis MA, McNamara JO, Roth BL. *Neuron.* 2009; 63:27–39. [PubMed: 19607790]
12. Brandao ML, Zanoveli JM, Ruiz-Martinez RC, Oliveira LC, Landeira-Fernandez J. *Behavioural brain research.* 2008; 188:1–13. [PubMed: 18054397]
13. Wilent WB, Oh MY, Bueteifisch CM, Bailes JE, Cantella D, Angle C, Whiting DM. *J Neurosurg.* 2010; 112:1295–1298. [PubMed: 19852539]
14. Berton O, McClung CA, Dileone RJ, Krishnan V, Renthal W, Russo SJ, Graham D, Tsankova NM, Bolanos CA, Rios M, Monteggia LM, Self DW, Nestler EJ. *Science.* 2006; 311:864–868. [PubMed: 16469931]
15. Ribeiro-Barbosa ER, Canteras NS, Cezario AF, Blanchard RJ, Blanchard DC. *Neuroscience and biobehavioral reviews.* 2005; 29:1255–1263. [PubMed: 16120464]

16. Langsrud O. *J Roy Stat Soc D-Sta.* 2002; 51:305–317.
17. Hsu SM, Raine L. *J Histochem Cytochem.* 1981; 29:1349–1353. [PubMed: 6172466]
18. Hancock JF, Cadwallader K, Paterson H, Marshall CJ. *EMBO J.* 1991; 10:4033–4039. [PubMed: 1756714]
19. Szymczak AL, Workman CJ, Wang Y, Vignali KM, Dilioglou S, Vanin EF, Vignali DA. *Nat Biotechnol.* 2004; 22:589–594. [PubMed: 15064769]
20. Pilpel N, Landeck N, Klugmann M, Seeburg PH, Schwarz MK. *J Neurosci Methods.* 2009; 182:55–63. [PubMed: 19505498]
21. Knobloch HS, Charlet A, Hoffmann LC, Eliava M, Khrulev S, Cetin AH, Osten P, Schwarz MK, Seeburg PH, Stoop R, Grinevich V. *Neuron.* 2012; 73:553–566. [PubMed: 22325206]
22. Franklin, KBJ.; Paxinos, G. *The mouse brain in stereotaxic coordinates.* Academic Press; San Diego: 1997.

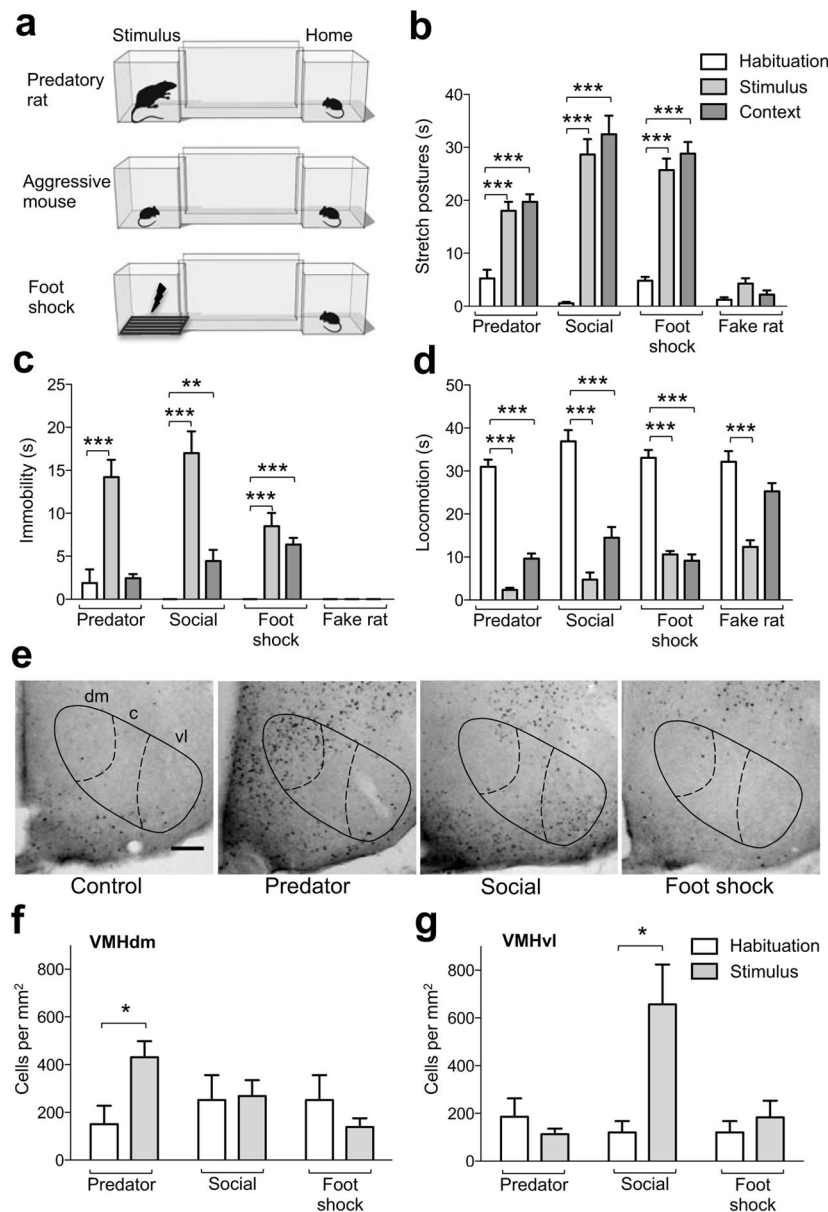


Figure 1. Similar fear behavior elicited in mice by different classes of threat

(a) The behavioral testing apparatus consisted of two chambers connected by a narrow corridor. An experimental mouse was continuously housed in one chamber (Home) and allowed to freely explore the corridor and second chamber (Stimulus) once daily for 20 minutes. At the end of the free exploration period on the fourth day, the door to the stimulus chamber was briefly closed to confine the mouse which was then exposed to either a predatory rat (Predator, < 5 s), aggressive mouse (Social, 10 min), electric foot shock (Foot shock, 1 min, 4 × 0.5 s, 0.5 mA), or toy rat (Fake rat, < 5 s) after which free exploration continued for an additional 10 minutes. Time spent performing (b) stretch postures, (c) immobility, and (d) locomotion was measured during the pre-stimulus (Habituation) and post-stimulus (Stimulus) free exploration periods, as well as on the day following stimulus

exposure (Context). Stretch postures and immobility were significantly increased after predator, aggressive conspecific, and foot shock, but not toy rat exposure when compared to the habituation session. Locomotion was significantly decreased after exposure to all stimuli. Re-exposure to the context elicited a significant increase in stretch postures and immobility and decrease in locomotion (Predator: N = 15, Social: N = 9, Foot shock: N = 6, Fake rat: N = 6, ** P < 0.01, *** P < 0.001). Quantification of c-Fos immunohistochemistry in brain sections from mice exposed to predator and aggressive conspecific in the two-chambered apparatus (e) revealed a significant increase in the number of c-Fos cells labeled in (f) VMHdm and (g) VMHvl, respectively, when compared to the habituation condition (Predator: N = 5, Social: N = 4, Foot shock: N = 3–4, * P < 0.05). Negligible neural activation was seen in VMH following foot shock exposure or in home cage control mice (scale bar = 50 μ m).

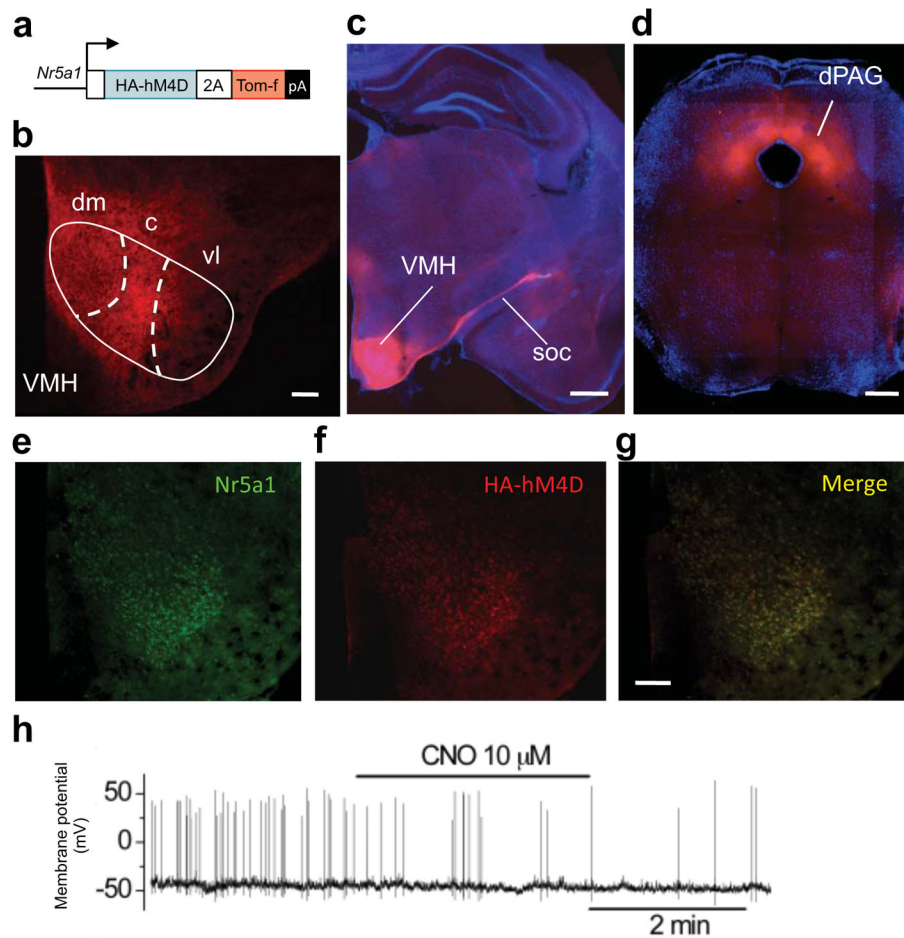


Figure 2. Generation and validation of *Nr5a1::hM4D-2A-tomatoF* transgenic mice
 (a) Mice carrying a transgene in which the HA-tagged hM4D pharmacogenetic neural inhibition tool and a farnesylated Tomato fluorescent protein (Tom-f) were expressed under control of the *Nr5a1* gene promoter showed expression of Tom-f in the (b) dorsomedial (dm) and central (c), but not ventrolateral (vl) divisions of the ventromedial hypothalamus (VMH), (c) in the supraoptic commissure (soc), and (d) in the dorsal periaqueductal gray (dPAG). Double immunofluorescence staining with (e) anti-*Nr5a1* and (f) anti-HA antibodies confirmed (g) selective and robust expression of the transgene in *Nr5a1* positive cells (scale bar = 100 μ m). (h) Sample trace from *in vitro* patch clamp electrophysiological recordings in VMHdm neurons confirmed a significant reduction of firing rate and membrane potential following CNO treatment in brain slices from *Nr5a1::hM4D-2A-tomatoF* mice but not control mice.

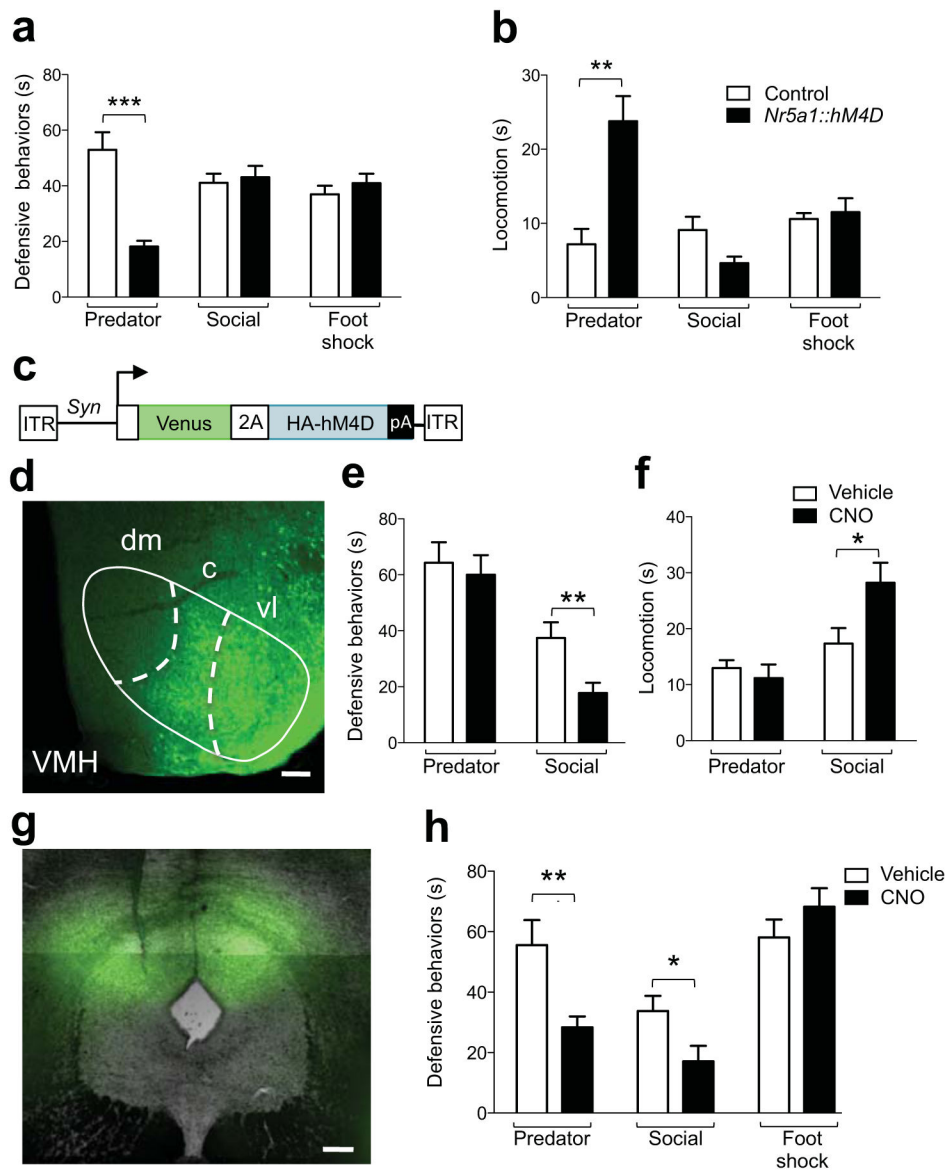


Figure 3. Functional dissociation of fear in VMH and PAG

Nr5a1::hM4D-2A-tomatoF transgenic mice, but not non-transgenic littermates showed a significant (a) inhibition of cumulative defensive responses and (b) increase of locomotion elicited by exposure to a predatory rat (Predator), but not an aggressive conspecific (Social), or electric foot shock (Foot shock, 4×0.5 s, 0.5 mA) following systemic administration of CNO (3 mg/kg, i.p., Predator: N = 7–8, Social: N = 7–8, Foot shock: N = 6–8). (c) Mice locally infected with an adeno-associated virus (AAV) expressing the Venus fluorescent protein and HA-tagged hM4D pharmacogenetic neural inhibition tool (HA-hM4D) under control of the *Synapsin* (*Syn*) gene promoter showed expression in the (d) ventrolateral (vl) VMH. AAV-*Syn::Venus-2A-hM4D* infected mice showed a significant (e) inhibition of cumulative defensive responses and (f) increase of locomotion elicited by exposure to an aggressive conspecific (Social), but not predatory rat (Predator) following systemic administration of CNO (3 mg/kg, i.p.) when compared to vehicle treated mice (Predator: N =

17–18, Social: N = 17–19). (g) Mice locally infected with AAV-Syn::Venus-2A-hM4D in the dorsal portion of the periaqueductal grey (dPAG) displayed a significant (h) decrease of cumulative defensive responses elicited by exposure to an aggressive conspecific (Social) or a predatory rat (Predator), but not to an electrical foot-shock (Foot shock, 4×0.5 s, 0.5 mA) following systemic administration of CNO (3 mg/kg, i.p.) when compared to similarly infected vehicle treated mice (Predator: N = 5–13, Social: N = 9–10, Foot shock: N = 13–14, * P < 0.05, ** P < 0.01, *** P < 0.001). Scale bar = 100 μ m.